European Radiology (2019) 29:1384–1390
https://doi.org/10.1007/s00330-018-5654-1

COMPUTED TOMOGRAPHY

Paper-based 3D printing of anthropomorphic CT phantoms: Feasibility of two construction techniques

Paul Jahnke[1] · Stephan Schwarz[1] · Marco Ziegert[1] · Felix Benjamin Schwarz[1] · Bernd Hamm[1] · Michael Scheel[1]

Received: 22 May 2018 / Revised: 27 June 2018 / Accepted: 4 July 2018 / Published online: 16 August 2018

Abstract

Objectives To develop and evaluate methods for assembling radiopaque printed paper sheets to realistic patient phantoms for CT dose and image quality testing.

Methods CT images of two patients were radiopaque printed with aqueous potassium iodide solution (0.6 g/ml) on paper. Two methods were developed for assembling the paper sheets to head and neck phantoms. (1) Printed sheets were fed to a paper-based 3D printer along with corresponding 3D printable STL files. (2) Paper stacks of 5-mm thickness were glued with toner, cut to the patient shape and assembled to a phantom. In a sample application study, both phantoms were examined with five different tube current settings. Images were reconstructed using filtered-back projection (FBP) and iterative reconstruction (AIDR 3D) with three strength levels. Dose length product (DLP), signal-to-noise ratios (SNR) and contrast-to-noise ratios (CNRs) were analysed. Data were analysed using 2-way analysis of variance (ANOVA).

Results Both methods achieved anthropomorphic phantoms with detailed patient anatomy. The 3D printer yielded a precise reproduction of the external patient shape, but caused visible glue artefacts. Gluing with toner avoided these artefacts and yielded more flexibility with regard to phantom size. In the sample application study, non-inferior SNR and CNR and up to 83.7% lower DLP were achieved on the phantoms with AIDR 3D compared with FBP.

Conclusions Two methods for assembling radiopaque printed paper sheets to phantoms of individual patients are presented. The sample application demonstrates potential for simulation of patient imaging and systematic CT dose and image quality assessment.

Key Points

- *Two methods were developed to create realistic CT phantoms of individual patients from radiopaque printed paper sheets.*
- *Analysis of five tube current and four reconstruction settings on two radiopaque 3D printed patient phantoms yielded non-inferior SNR and CNR and up to 83.7% lower dose with iterative reconstruction in comparison with filtered back projection.*
- *Radiopaque 3D printed phantoms can simulate patients and allow systematic analysis of CT dose and image quality parameters.*

Keywords Printing · Three-dimensional · Phantoms, imaging · Tomography, X-ray computed

Abbreviations

AIDR 3D	Adaptive iterative dose reduction 3D
ANOVA	Analysis of variance
ATCM	Automated tube current modulation
CCA	Common carotid artery
CT	Computed tomography
CNR	Contrast-to-noise ratio
dFOV	Display field of view
DLP	Dose length product
FBP	Filtered back projection
HU	Hounsfield units
LOM	Laminated object manufacturing
R3P	Radiopaque 3D printing
ROI	Region of interest
SD	Standard deviation
SNR	Signal-to-noise ratio

Electronic supplementary material The online version of this article (https://doi.org/10.1007/s00330-018-5654-1) contains supplementary material, which is available to authorized users.

✉ Paul Jahnke
paul.jahnke@charite.de

[1] Department of Radiology, Charité – Universitätsmedizin Berlin, Corporate Member of Freie Universität Berlin, Humboldt-Universität zu Berlin, and Berlin Institute of Health, Charitéplatz 1, 10117 Berlin, Germany

Introduction

Investigation of dose-reduction techniques can be challenging on geometrically simple, uniform phantoms and require an environment more representative of the clinical imaging situation [1, 2]. For example, tube current and voltage settings are frequently investigated in clinical trials on patient populations [3–5]. However, study designs involving patients are subject to poor standardization, limited availability of study participants and the impossibility of repeated exposure of individual subjects for systematic investigations. All of these challenges could be addressed by realistic patient phantoms.

Radiopaque 3D printing (R3P) was recently introduced and has the potential to provide such phantoms. Phantoms are generated by directly printing patient CT images with radiopaque ink on paper and stacking the printed sheets [6]. R3P avoids segmentation-related loss of information between the CT data set and the phantom, allows adjustment of attenuation for all tissues through printer deposition and uses low-cost materials and equipment. Feasibility for creating patient individual CT phantoms has been demonstrated, and recently Ikejimba et al used this method to create a highly realistic phantom for breast imaging [7].

The previously published R3P methods were confined to stacking loose radiopaque printed paper sheets, but did not generate mechanically stable phantoms with realistic external shapes. Further development should therefore aim at cutting and gluing the printed papers to generate stable phantoms with the shape of the patient. Two different approaches were considered to achieve these goals: (1) a paper-based 3D printer and (2) a customized laminated object manufacturing (LOM) procedure, where adhesive-coated layers are cut and glued together to generate 3D objects [8]. The aim of this study was to develop and evaluate these methods for assembling radiopaque printed paper sheets to realistic patient phantoms for CT dose and image quality testing.

Materials and methods

Study design

The institutional review board approved the study and written informed consent was obtained from the patients. CT angiography images of two patients were radiopaque printed with aqueous potassium iodide solution (0.6 g/ml) on 80 g/m^2 paper as recently described [6], resulting in stacks of 2,164 printed sheets for Phantom 1 and 2,295 printed sheets for Phantom 2. Two methods were developed for assembling the printed sheets to head and neck phantoms using (1) a paper-based 3D printer and (2) a customized LOM method. Head and neck phantoms were selected to fit the build size of the paper-based 3D printer.

Phantom 1 – Mcor Iris 3D printer

The *Mcor Iris* 3D printer (*Mcor Technologies*, retail price 35,000 euros) automatically stacks, cuts and glues standard office paper in three steps: (1) A paper sheet is pulled from the paper tray on the build platform and heat compressed against the layer underneath. (2) The paper is cut with a blade. (3) Glue is deposited in lines on the paper in preparation for the next layer. The CT images were processed to a printable 3D model adapted to the requirements of the *Mcor Iris* using *Mimics Innovation Suite (Materialise)*, a *Python* script and *OpenSCAD*. A 3D model consisting of the external patient contour was generated from the CT images and exported as an STL file. The model was centred to the point of origin, cropped in the x and y dimension to fit the 3D printer's build size and divided into four subparts. The radiopaque printed paper sheets were loaded into the paper tray of the *Mcor Iris*. The STL files of all four model subparts were subsequently imported to the 3D printer's *SliceIT* software and printed. The final 3D model was assembled by applying a thin layer of glue on top of each subpart and compressing the subparts for 24 h (Fig. 1).

Phantom 2 – customized laminated object manufacturing

A customized LOM procedure was developed, consisting of (1) heat gluing small paper stacks with toner to stable subparts, (2) cutting every subpart to the patient shape and (3) assembling the subparts to the final phantom. First black laser toner was printed on the blank side of the radiopaque printed paper sheets using a full black rectangular print template and a *Xerox Phaser 7100* laser printer *(Xerox Corporation)*. Stacks of 50 paper sheets per stack were heat pressed at 115°C and 4 bar for 15 min per stack (temperature, pressure and time were set on the heat press). As a result, the paper sheets of every stack were glued together, yielding stable subparts of 5-mm thickness. Next, the external patient contour was generated with the *OpenCV* library in *Python* for every subpart using threshold values and the maximum dimensions of the corresponding CT images. The contour files were used for laser cutting the corresponding subparts to the external patient contour. Finally, the subparts were stacked, compressed at 7.7 bar with a hydraulic press (pressure measured by the press) and heated at 115°C for 72 h in a preheated oven (temperature and time set on the oven). After cooling to room temperature, remaining waste paper material was removed to unwrap the final phantom (Fig. 2).

CT dose and image quality

Both phantoms were examined on a *Canon Aquilion Prime* CT scanner *(Canon Medical Systems)*. The tube potential was

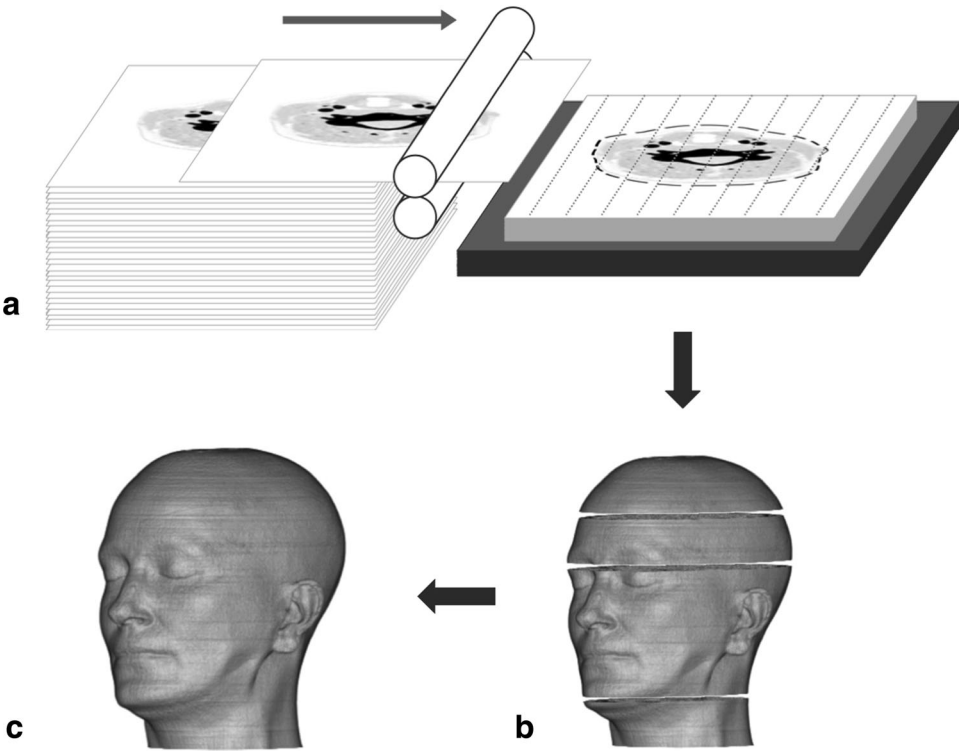

Fig. 1 Phantom manufacturing with the paper-based 3D printer. Paper sheets were pulled from a paper tray, glued to the layer underneath, cut to the patient shape and coated with glue arranged in lines in preparation for the next layer (**a**). Four subparts were created (**b**) and assembled to the final phantom (**c**)

120 kVp. The tube current was set to fixed 10 mA and automated tube current modulation (ATCM) with SD values of 7.5, 10, 14 and 18. Filtered-back projection (FBP) and adaptive iterative dose reduction 3D (AIDR 3D) with three different strength settings (mild, standard and strong) were used for image reconstruction. The dose length product (DLP) was registered. ROIs were placed in six consecutive slices in the left and right common carotid artery (CCA), adipose tissue and in the display field of view (dFOV) outside the phantoms for background noise. Signal-to-noise ratios (SNRs) were calculated by dividing mean CCA ROI HU by the standard deviation of the background noise. Contrast-to-noise ratios were calculated by dividing the difference between CCA and adipose HU by the standard deviation of the background noise.

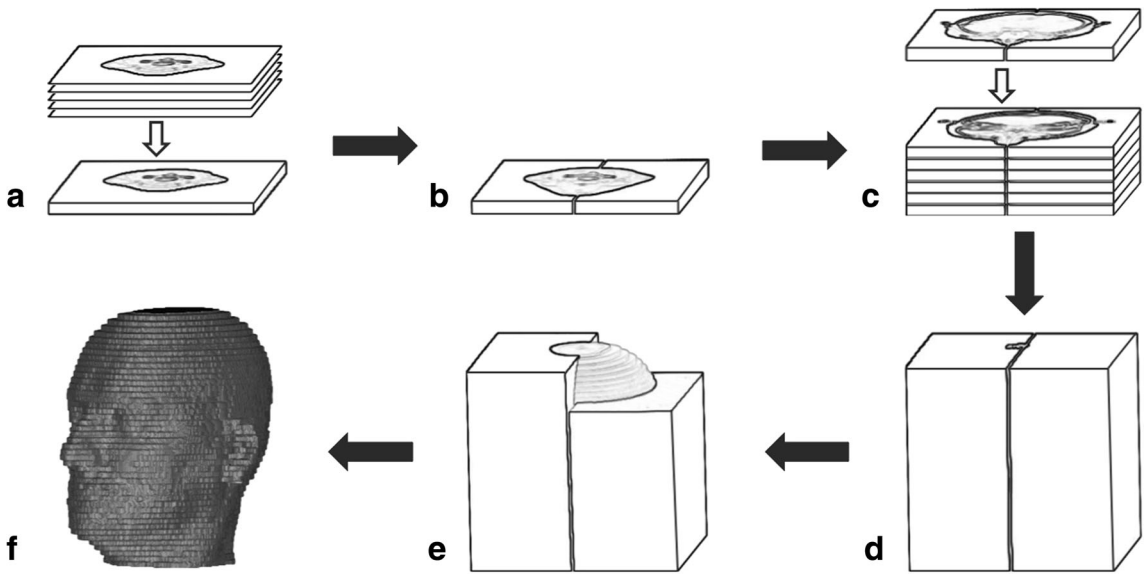

Fig. 2 Phantom manufacturing with the customized laminated object manufacturing procedure. Toner-coated paper sheets were stacked and glued to 5-mm thick subparts (**a**). The subparts were cut to the patient shape (**b**), stacked (**c**) and glued together (**d**). Overhanging waste paper was removed (**e**) to unwrap the final phantom (**f**)

Statistical analysis

SNR and CNR values between all methods were compared using 2-way analysis of variance (ANOVA) of tube current and reconstruction method. Differences were interpreted as significant when $p < 0.05$.

Results

Phantom 1 – Mcor Iris 3D printer

The phantom assembled with the *Mcor Iris* 3D printer is shown in Fig. 3. The printer allowed automatic paper processing and precise 3D printing (machine axis resolution as specified by the manufacturer 12 × 12 × 100 μm^3 for x, y and z). Manual work was limited to loading the paper tray, which could hold up to 1,500 paper sheets. The build volume dimensions of the 3D printer were limited to 256 × 169 × 150 mm^3 (x, y and z). As a consequence, the right phantom ear had to be cropped and the phantom was divided into subparts. There were offsets ≤ 1 mm between the stacked paper sheets. The glue lines deposited by the printer on every paper sheet were visible in the CT images of the phantom.

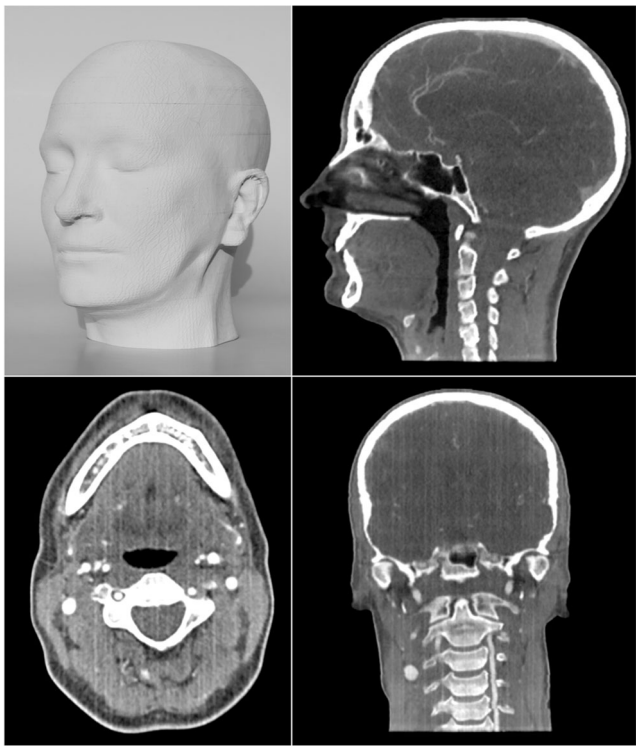

Fig. 3 Phantom 1 manufactured with the paper-based 3D printer (acquisition with automated tube current modulation (ATCM), SD 7.5 and adaptive iterative dose reduction 3D (AIDR) 3D mild). Every paper sheet was cut to the patient shape. The papers were glued together with glue arranged in lines, which caused imaging artefacts, visible as numerous parallel vertical lines

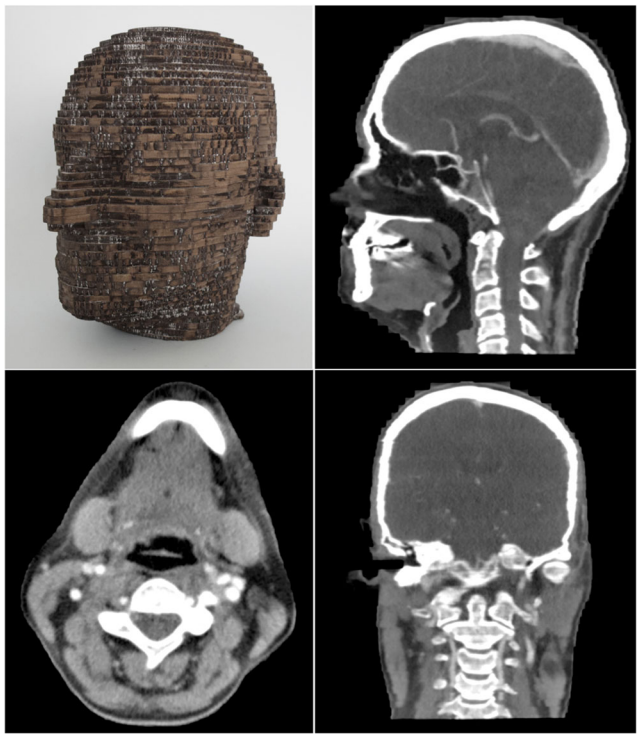

Fig. 4 Phantom 2 manufactured with the customized laminated object manufacturing procedure (acquisition with automated tube current modulation (ATCM), SD 7.5 and adaptive iterative dose reduction 3D (AIDR) 3D mild). Toner-coated paper sheets were glued to 5-mm thick subparts. The subparts were cut to the patient shape, stacked and glued together. Image quality was not impaired by glue artefacts

Phantom 2 – customized laminated object manufacturing

Figure 4 shows the phantom manufactured using the LOM procedure. In total, 15 toner cartridges were used, and toner costs added up to approximately 600 euros. The level of detail of the phantom shape was determined by the thickness of the subparts. Five-mm thickness, corresponding to 50 paper sheets, allowed a reasonable compromise between phantom shape resolution and the number of subparts that had to be cut to the patient shape. The CT images of the phantom showed small overhanging blank paper areas outside the radiopaque printed patient body. These were due to the export of the maximum patient contour of the corresponding CT images, which allowed avoiding cutting of radiopaque printed areas. Standard A4 paper provided enough space for printing and assembling the entire phantom at the original size of the patient. Offsets ≤ 2 mm between some subparts were caused by imprecise stacking of the subparts. There were no visible imaging artefacts attributable to the gluing of the papers, as the papers were homogeneously coated with the toner, which served as glue.

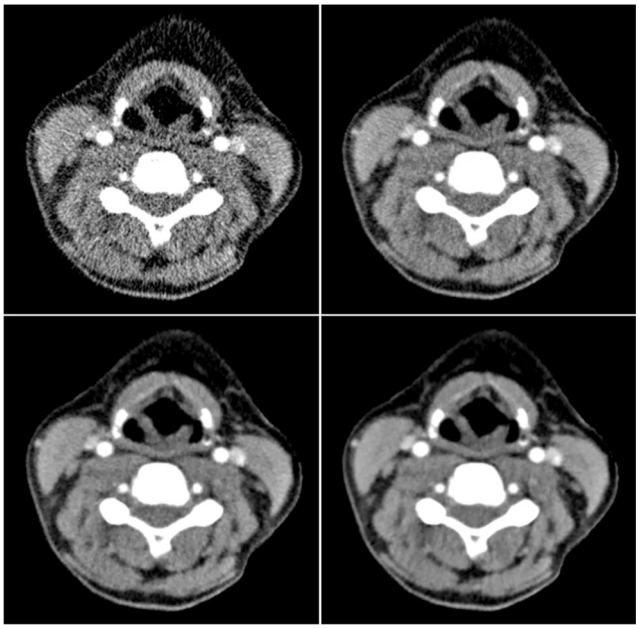

Fig. 5 Exemplary sequence of image acquisitions performed on Phantom 2. **Top left:** 10 mA, filtered back projection (FBP). **Top right:** Automated tube current modulation (ATCM) Standard, FBP. **Bottom left:** ATCM Standard, adaptive iterative dose reduction 3D (AIDR) Standard. **Bottom right:** ATCM High Quality, AIDR Strong

CT dose and image quality

Figure 5 shows an exemplary series of acquisitions performed with Phantom 2. SNR values of both phantoms are displayed in Fig. 6. Increasing tube current and associated DLP values resulted in significantly higher SNR and CNR values ($p < 0.0001$). SNR and CNR values were significantly higher for AIDR 3D than for FBP and increased with increasing AIDR 3D strength setting ($p < 0.0001$). The maximum dose reduction potential with non-inferior SNR and CNR was 82.5% for Phantom 1 and 83.7% for Phantom 2 (FBP, ATCM High Quality vs. AIDR 3D Strong, ATCM Low Dose). Compared with AIDR 3D Standard, the dose reduction potential decreased to 64% for Phantom 1 and 65.8% for Phantom 2 (FBP, ATCM High Quality vs. AIDR 3D Standard, ATCM Standard).

Discussion

Two methods were developed to create realistic CT phantoms of individual patients from radiopaque printed paper sheets. The first method used a paper-based *Mcor* 3D printer. The second method used toner from a laser printer for gluing the printed sheets. A sample application study on these phantoms demonstrated potential of up to 83.7% dose reduction and non-inferior SNR and CNR with AIDR 3D vs. FBP on a *Canon Aquilion Prime* CT scanner.

The *Mcor* 3D printer provided a fully developed system that could automatically perform all steps for assembling paper sheets to a 3D object. However, the build size was below A4 paper size and artefacts were caused by the glue lines deposited on every paper sheet. Lowering the printer's glue deposition or using a different glue with lower attenuation may reduce these artefacts, but also impair phantom stability or cause printer malfunction (effects not investigated in this study). To overcome these limitations, a second method was developed that (1) offered more flexibility of paper size, (2) avoided artefacts related to gluing the papers, and (3) did not require use of a 3D printer. This method made use of a heated toner to glue layers together, a technique that was previously used in commercial LOM machines to glue paper sheets [8]. For the purposes of this work, a standard office laser printer was sufficient to coat the sheets with toner and glue the papers without impairing the image quality through visible glue artefacts. The authors therefore favoured Phantom 2 manufactured with the LOM method. Larger phantoms may be achieved in the future by connecting parts manufactured

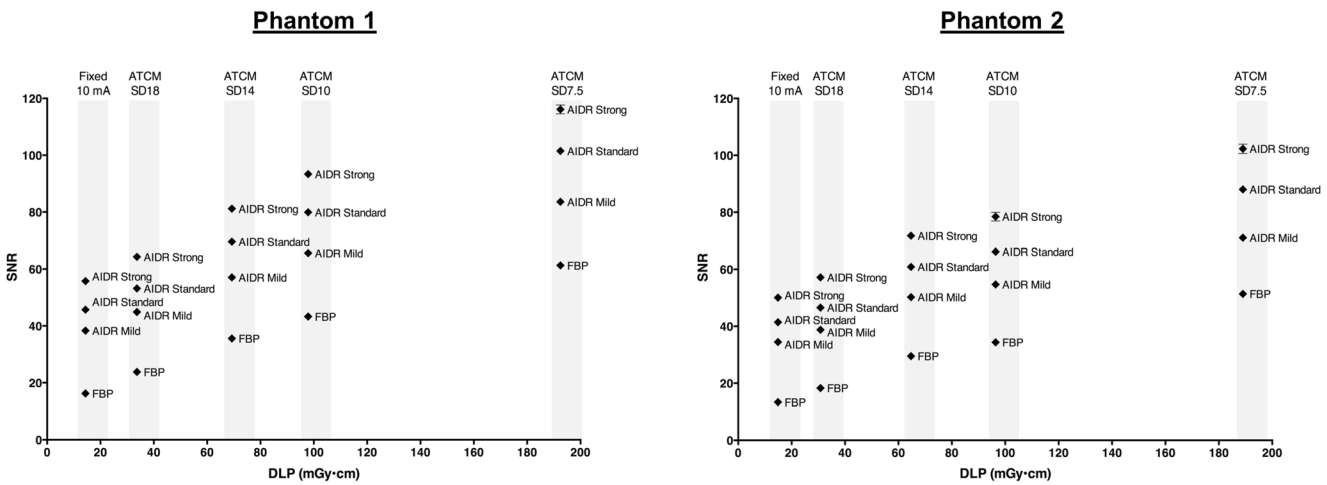

Fig. 6 SNR values for Phantom 1 (left) and Phantom 2 (right). Mean ± SD values of 12 measurements in the left and right common carotid artery (CCA)

with either method to a larger phantom or using larger paper sizes, which is only applicable to the LOM method.

Previous work used UV-curable polymer, material extrusion, selective laser sintering and powder-based 3D printers to create CT phantoms [9–13]. However, with commercial 3D printers modifications of the printing processes and build material attenuation properties are restricted [13]. Data segmentation is necessary and causes loss of information between the template CT data set and the phantom [14]. In contrast to these previous approaches, radiopaque 3D printing controls phantom attenuation in a first 2D printing step and assembles the printed sheets to a phantom in a second 3D stacking step. Accuracy of radiopaque 2D printing for simulation of low and high attenuating tissues was previously demonstrated [6, 7]. The present work complements the method and provides two approaches for assembling the printed sheets to patient phantoms. To the authors' knowledge, there are currently no other phantoms replicating patients at a comparable level of detail.

The phantoms developed in this work provided a realistic simulation of clinical head and neck imaging and allowed systematic investigation of dose and imaging parameters. This is of particular relevance because phantom shape, size, texture and heterogeneity can influence physical image properties (e.g. noise and resolution) and task-based CT system performance evaluation [1, 2, 10]. Evaluation of clinical CT imaging and dose reduction techniques should therefore be performed in a realistic clinical context rather than on simplified phantoms [15]. The 83.7% dose reduction potential of AIDR 3D with non-inferior SNR and CNR observed in this study on two patient phantoms was slightly above the findings of > 70% in a previous patient trial on the same CT system [16]. However, the authors of this previous study did not provide the strength setting that was used. Compared with the standard AIDR 3D strength setting, the dose reduction observed in the present study decreased to 65.8%.

The limitations of this study are that only one phantom was investigated per method and reproducibility was not demonstrated. While the sample application study showed potential for dose reduction, the results were not directly compared with clinical results assessed on patients. Also, the results could not be directly compared between the two phantoms, as two different patients were selected as template for phantom manufacturing.

Two methods are presented to create phantoms of individual patients from radiopaque printed paper sheets. The first method used a paper-based 3D printer and allowed automatic processing. The second method used a customized LOM approach and avoided glue-related image artefacts. The sample application study demonstrated dose reduction potential on these phantoms within the range of clinical observations. Radiopaque 3D printed phantoms can simulate patients and allow systematic investigation of dose and image quality in computed tomography.

Acknowledgements The authors would like to acknowledge the assistance of Asmaa Shatir, Department of Radiology, Charité – Universitätsmedizin Berlin, corporate member of Freie Universität Berlin, Humboldt-Universität zu Berlin, and Berlin Institute of Health, Charitéplatz 1, 10117 Berlin, Germany.

Funding This study has received funding by the Bundesministerium für Wirtschaft und Energie (DE): 03EFHBE093.

Compliance with ethical standards

Guarantor The scientific guarantor of this publication is Dr. Paul Jahnke.

Conflict of interest The authors of this manuscript declare no relationships with any companies whose products or services may be related to the subject matter of the article.

Patents Patent applications for the 3D printing method were filed by Dr. Jahnke and PD Dr. Scheel: DE202015104282U1, EP000003135199A1, US020170042501A1.

Statistics and biometry No complex statistical methods were necessary for this paper.

Informed consent Written informed consent was obtained from the patients.

Ethical approval Institutional Review Board approval was obtained.

Methodology
- Prospective
- Experimental
- Performed at one institution

References

1. Solomon J, Ba A, Bochud F, Samei E (2016) Comparison of low-contrast detectability between two CT reconstruction algorithms using voxel-based 3D printed textured phantoms. Med Phys 43: 6497
2. Solomon J, Wilson J, Samei E (2015) Characteristic image quality of a third generation dual-source MDCT scanner: Noise, resolution, and detectability. Med Phys 42:4941–4953
3. Lee KH, Lee JM, Moon SK et al (2012) Attenuation-based automatic tube voltage selection and tube current modulation for dose reduction at contrast-enhanced liver CT. Radiology 265:437–447
4. Kanematsu M, Kondo H, Miyoshi T et al (2015) Whole-body CT with high heat-capacity X-ray tube and automated tube current modulation–effect of tube current limitation on contrast enhancement, image quality and radiation dose. Eur J Radiol 84:877–883
5. Nakaura T, Nakamura S, Maruyama N et al (2012) Low contrast agent and radiation dose protocol for hepatic dynamic CT of thin adults at 256-detector row CT: effect of low tube voltage and hybrid iterative reconstruction algorithm on image quality. Radiology 264: 445–454
6. Jahnke P, Limberg FR, Gerbl A et al (2017) Radiopaque Three-dimensional Printing: A Method to Create Realistic CT Phantoms. Radiology 282:569–575

7. Ikejimba LC, Graff CG, Rosenthal S et al (2017) A novel physical anthropomorphic breast phantom for 2D and 3D x-ray imaging. Med Phys 44:407–416
8. Chua CK, Leong KF (2014) 3D Printing and Additive Manufacturing: Principles and Applications, 4th edn. World Scientific Publishing, Singapore
9. Leng S, Chen B, Vrieze T et al (2016) Construction of realistic phantoms from patient images and a commercial three-dimensional printer. J Med Imaging (Bellingham) 3:033501
10. Solomon J, Samei E (2014) Quantum noise properties of CT images with anatomical textured backgrounds across reconstruction algorithms: FBP and SAFIRE. Med Phys 41:091908
11. Yoo TS, Hamilton T, Hurt DE, Caban J, Liao D, Chen DT (2011) Toward quantitative X-ray CT phantoms of metastatic tumors using rapid prototyping technology. 2011 IEEE International Symposium on Biomedical Imaging: From Nano to Macro 1770–1773
12. Hazelaar C, van Eijnatten M, Dahele M et al (2018) Using 3D printing techniques to create an anthropomorphic thorax phantom for medical imaging purposes. Med Phys 45:92–100
13. Ceh J, Youd T, Mastrovich Z et al (2017) Bismuth Infusion of ABS Enables Additive Manufacturing of Complex Radiological Phantoms and Shielding Equipment. Sensors (Basel) 17:459
14. Ionita CN, Mokin M, Varble N et al (2014) Challenges and limitations of patient-specific vascular phantom fabrication using 3D Polyjet printing. Proc SPIE Int Soc Opt Eng 9038:90380M
15. Solomon J, Marin D, Roy Choudhury K, Patel B, Samei E (2017) Effect of Radiation Dose Reduction and Reconstruction Algorithm on Image Noise, Contrast, Resolution, and Detectability of Subtle Hypoattenuating Liver Lesions at Multidetector CT: Filtered Back Projection versus a Commercial Model-based Iterative Reconstruction Algorithm. Radiology 284:777–787
16. Yu S, Zhang L, Zheng J, Xu Y, Chen Y, Song Z (2017) A comparison of adaptive iterative dose reduction 3D and filtered back projection in craniocervical CT angiography. Clin Radiol 72:96 e1-96.e6